

Disruption of *Staphylococcus aureus* Biofilms with Purified *Moringa oleifera* Leaf Extract Protein

**Lakshmi Menon¹, Omprakash Chouhan¹, Rushikesh Walke¹, Shruti Shah², Samir Damare^{2§},
Sumit Biswas*^{1#}**

¹ ViStA Lab, BITS, Pilani – KK Birla Goa Campus, Zuarinagar, Goa 403726, India.

²Biological Oceanography Division, CSIR- National Institute of Oceanography, Dona Paula, Goa, India.

§ORCID ID: 0000-0002-4201-4844

#ORCID ID: 0000-0002-4945-3030

*Corresponding author Email: sumit@goa.bits-pilani.ac.in

Phone: +91 832 2580178

Abstract:

Background: A major cause of economic losses, in the medical implant sector has been bacterial biofilms due to their abilities to persist on various surfaces and their tolerance against endogenous defences, antibiotics, or other anti-microbial agents. The quest for potential sources causing inhibition or disruption of bacterial biofilms has been taken up to alleviate the loss. Plant-derived extracts such as essential oils, bioactive compounds and other solvent extracts are regularly being put to use instead of antibiotics and other synthetic compounds as they are safer, economical, and in many instances, have an elaborate history of traditional medicinal usage.

Objectives: As a plant that has been traditionally used over the centuries, the *Moringa oleifera* Lam., or more commonly the drumstick tree, is being tapped for myriad pharmaceutical applications. The protein-rich leaf of this tree has not only proved to be of great nutritional value, but also divulged numerous potential therapeutic applications.

Methods: While reports of proteinaceous components are rare, here we report the efficacy of the aqueous extract of the leaf of *M. oleifera* and a 62 kDa protein component in the disruption of staphylococcal biofilms, which are largely implicated in nosocomial infections.

Results and Conclusion: The application of the *M. oleifera* leaf extract protein had a marked effect on the biofilm growth or formation by *Staphylococcus aureus*. While the crude extract itself showed considerable disruption of biofilm formation, the application of the purified protein obtained after a two-step process led to a significant increase in the anti-biofilm activity.

Keywords: Biofilm, *Moringa oleifera*, leaf extract, *Staphylococcus aureus*, Crystal violet, SEM

1. Introduction:

Associated with more than 80% of pathogenic infections [1], biofilms are sessile bacterial communities that grow in close association and adhere to any inert surface, epithelial layer or even a water interface. Adding to the complexity is the dense matrix of the biofilm, made of extracellular polymeric substance (EPS) or exopolysaccharide that provides a conducive environment for cell growth and enhanced tolerance [2]. Such biofilms have a mechanism to protect the community in it by allowing the release of efflux pumps and enzymes (like β -lactamase) for expulsion or disruption of antibiotics from the cell [3, 4]. A number of gram positive and gram-negative bacteria form biofilms, of which *Staphylococcus aureus* and *Pseudomonas aeruginosa* are the most dominant, originating mostly as nosocomial infections via surgical implants, prosthetic valves and venous catheters [5-8].

Plant-derived extracts like *Piper longum* against *Streptococcus pyogenes* [9], *Terminalia catappa* [10], *Murraya koenigii* and *Euphorbia hirta* against *P. aeruginosa* [11, 12], or *Allium sativum* against *S. aureus* [13], have had a long history of reported anti-bacterial activities. *Moringa oleifera* Lamarck, commonly known as the drumstick tree or the horseradish tree, is a phanerogamous plant, native to tropical regions of South Asia [14, 15]. Every part of this tree – be it the seeds or pods or the leaves – has been traditionally used to treat various physiological conditions and diseases. These diseases range from gastric ulcers to diabetes, hypertension, cancer, liver disease, etc. Almost all the plant parts have now been found to be rich in bio-actives [16-20], but the complete evaluation and analysis of these bioactives is something which has been missing. When it comes to looking for protein components, the gap in knowledge is even more stark.

While the activities of the methanolic and ethanolic extracts of *M. oleifera* leaves have been reported abundantly [21, 22], only recent reports have shed light on the efficacy of aqueous extracts (containing proteinaceous components) of the leaves compared to traditional antibiotics [23]. The crude aqueous extract of *M. oleifera* leaves was found to display enhanced inhibition halos on *S. aureus*, *Aeromonas caviae*, *Vibrio parahaemolyticus* and *Enterococcus faecalis* cultures [24]. However, there are hardly any reports of the specific activity of the leaf extracts against bacterial biofilms till date [8]. The anti-biofilm potential of the plant has only been reported for the seed coat, which has been used against *S. aureus* biofilm contamination in dairy effluents [25, 26]. *M. oleifera* leaves have been known to be rich in protein content – in fact, an analysis of the protein content in dried *M. oleifera* leaves reported nine times higher concentration of protein than yoghurt [27, 28].

Based on the available literature, this study attempted to elucidate the effects of *M. oleifera* aqueous leaf extract on *S. aureus* biofilms and configure the properties of the principal component. The preliminary results of the crude extract against staphylococcal biofilms showed encouraging activity using the novel methodology developed by our group for visualizing biofilm disruptions under the scanning electron microscope. Further purification of the crude aqueous extract according to our previous protocol yielded a protein-rich fraction [29]. Application of the purified protein on the staphylococcal biofilm displayed enhanced disruption of the biofilm almost to the level of abolition. Even the exopolysaccharides sticking to the coccal surfaces were drastically reduced, as was visible in the SEM images. The protein was characterized to be a monomer with molecular weight of 62 kDa and its partial sequence done with MS-MS sequencing revealed its novel status. The protein was stable till a temperature of 50°C, and showed typical amid peaks in the FTIR spectrum. The minimum inhibitory concentration of this protein was found to be 100 µg/ml. The pronounced effect of the *M. oleifera* leaf protein, referred to as p62, on the biofilms of *S. aureus* was well demonstrated by both confocal and electron microscopy.

2. Materials and Methods

2.1. Extraction from Moringa oleifera leaf

Mature leaves of *M. oleifera* Lam., belonging to the family Moringaceae, were hand-picked from BITS, Mormugao, South Goa, India and dried under shade for 2 weeks. The voucher specimen in the form of the herbarium is maintained in the Calcutta University Herbarium (CUH/20088). The leaves were ground into a fine powder in a mortar and pestle after complete drying and readied for extraction [29]. The powdered leaves were stored at room temperature (25±2°C) in a dry, air tight container at a dark place until further use. For extraction, 1g of *M. oleifera* leaf powder was dissolved in 6 ml (1:6 w/v) of extraction buffer (10mM of Potassium Phosphate Buffer, pH 7.0) along with freshly prepared 10mM protease inhibitor, phenylmethylsulphonyl fluoride (PMSF, Sigma-Aldrich, Germany). The entire mixture was vortexed and allowed to dissolve, followed by centrifugation at 10,000 rpm at 4°C for 20 minutes. The supernatant (crude extract) was carefully collected and stored at 4°C for immediate use and -20° C for prolonged storage.

The crude extract was subjected to further purification with ammonium sulphate (Merck, Germany) precipitation until 50% saturation was obtained, followed by centrifugation and collection of the precipitated protein pellet and supernatant. Both the fractions were dialysed overnight in a 12 kDa dialysis membrane against the extraction buffer, to ensure removal of any components smaller than 12 kDa and stored as fractions S (supernatant) and P (pellet) at 4°C until use. The extracts at each

stage were estimated for presence of protein in a 10% SDS-PAGE. The fraction P was further purified by gel filtration chromatography using a Superdex 200 prep grade column in an ÄKTA Pure FPLC system (GE Healthcare Life Sciences). The purified fractions were collected, pooled and dialysed overnight in buffer (20 mM KCl, 20mM Potassium Phosphate buffer). The appearance of more than one band led us to further purify the fractions in a Q HP column (GE Healthcare Life Sciences) using appropriate salt gradient.

2.2. Characterization of the Purified Protein Fraction

2.2.1. Minimum Inhibition Concentration (MIC)

The MIC against *S. aureus* was determined as per the method reported in Liu et al. 2017 [30]. *S. aureus* culture was grown overnight at 37°C in LB media and diluted to an OD₆₀₀ of 0.1, from which 200µl was added to a 96 well plate and incubated at 37°C for 6 hours. After 6 hours, the wells were treated with different concentrations of p62 protein (200, 100, 80, 60 and 40µg) along with positive and negative control. In this study, lysostaphin (5µg) was used as the positive control and Proteinase K-digested p62 protein was used as negative control. After the treatment, the plate was incubated further at 37°C for 6, 12 and 24 hours and OD values were measured at the end of the incubation period in a microplate reader (MULTISKAN GO, Thermo).

2.2.2. Determination of Oligomeric Status

The oligomeric status of the protein was determined by performing size exclusion chromatography using a Superdex 200 column (GE Healthcare) and standard gel filtration markers kit (Sigma Aldrich). The column was washed with 20% ethanol and equilibrated with potassium phosphate buffer (50mM KCl, 20mM potassium phosphate pH 7.4). The lyophilized protein markers were dissolved in the same buffer as per the concentrations mentioned in the kit and was injected into the FPLC system (ÄKTA Pure) at a flow rate of 0.8 ml/minute. The protein markers ranging from 200 kDa (Blue Dextran) to 12.4 kDa (Cytochrome c) were run through the column and the void volume (V_0) and elution volume (V_e) were estimated. The retention volumes for each of the proteins in the marker were noted and used to derive the retention factor (R_f). The retention factor is defined by the following equation:

$$R_f = (V_e - V_0) / (V_t - V_0), \text{ where } V_t \text{ is the geometric bead volume of the column}$$

The purified p62 was also injected into the column at the same flow rate. The peaks obtained during the separation were evaluated for elucidating the oligomeric status.

2.2.3. FTIR

FTIR spectroscopic scans for purified fractions of the p62 protein were also performed [31]. The secondary structure of the protein was quantified by the presence of characteristic amide bands across a wavelength of 900-2100 nm. 0.25 µg of the p62 protein was loaded onto the sample holder and analysed in an IR spectrophotometer (Perkin Elmer Spectrum IR Version 10.6.1).

2.2.4. Sequence Determination Using Mass Spectrometric Analysis

For determining the protein sequence of the 62 kDa protein, the protein band was excised aseptically from the de-stained SDS PAGE gel and was subjected to in-gel digestion [32]. Digested sample was acidified by formic acid and centrifuged at 14000 rpm, 28°C for one minute. 10 µl of the digested sample was transferred to the MS vial while the remaining sample was frozen at -20 °C. Mass spectrometric analysis of the protein sample was performed on 6538 UHD LC MS QTOF (Agilent Technologies, USA). Briefly, 5 µL tryptic digests were loaded onto the SmMol-Chip-43 II 80A C18 43mm col. (Agilent Technologies, USA) using 1260 Infinity Cap pump (Agilent Technologies, USA) with 97 % acetonitrile. Separation of the ions was done onto the column using 1260 Infinity Nano pump (Agilent Technologies, USA) with a non-linear gradient of 3-90% acetonitrile for 57 minutes. Formic acid was used as an adduct in both solvents (acetonitrile and sterile 0.22 µm filtered de-ionised water). Samples were run in positive polarity for 57 minutes. The raw spectral data (.d file) was analysed using Spectrum Mill Workbench B.

2.2.5. Stability with respect to temperature

The intrinsic fluorescence emitted by the protein was quantified in a spectrofluorometer (Jasco, FP-8200) at varying temperatures. The purified p62 protein extract was tested for temperature profiles of 25, 30, 37, 50 and 60°C respectively. The sample was excited at 295 nm and a spectral graph was obtained at the emission range of 310-450 nm.

CD analysis of the protein sample was performed in terms of varying temperature. For temperature analysis, the protein samples were incubated for 10 minutes at temperatures 4, 25, 37, 42 and 50°C, followed by measurement of the CD signal in the CD spectropolarimeter (Jasco J-815 Circular Dichroism Spectropolarimeter). The secondary structure was explored by an in-software CD de-convoluter and values were considered as per Reed's reference.

2.3. *Growth of S. aureus biofilms*

Bacteria (*S. aureus* RN322) were first allowed to grow in liquid medium at 37°C for 24 hours with continuous shaking at 120 rpm. After sufficient growth, culture tubes were transferred to static conditions (without any disturbance) and incubated for 5 days at 37°C. Growth was

checked at an interval of 2 days to make sure that a dense mat of the biofilm was formed. A sterile glass coverslip (20 mm x 20 mm) was introduced to the culture at the air-liquid interface to transfer the biofilms from liquid media to the glass coverslips. Glass coverslips with microbial biofilms were gently washed with 1X PBS, to ensure removal of any unattached or loosely attached bacterial cells.

2.4. Assay for Biofilm Formation

Biofilm formation assay was performed according to the established method [33] with minor modifications as described before [34]. In this protocol, 1% of an overnight bacterial culture was transferred to fresh LB broth in glass tubes and incubated at 37°C with shaking at 120rpm for 12h. Post this initial incubation, all the tubes were transferred to static conditions and checked for the development of slimy film or pellicles at the air-liquid interface, implying the formation of the biofilm. For staining with 0.2% crystal violet, the media was carefully removed from the tubes and the bacterial cells bound to the walls stained with the dye for 5 min at room temperature. The tubes were then rinsed with distilled water to remove any unbound crystal violet and air dried before imaging. For quantitative estimation using a spectrophotometer, the biofilm was dissolved in 75% ethanol and OD₅₇₀ was noted. For each experiment, three sets were replicated to allow for observation of pellicles from the first to the seventh day.

The partially purified protein fraction from the gel filtration (150µg/ml) and the purified fraction (after ion exchange) (100µg/ml) were both used to treat the biofilms before assaying for crystal violet binding. Negative controls in the form of proteinase K-treated samples, lysostaphin-treated samples as positive control and blank buffer were also used to check the effect on the biofilms formed. The proteinase K-digested extracts were suitably treated after optimized time interval to prevent any residual activity of proteinase K on the biofilm. We used parametric method t-test with equal variance for the control and treated samples. The statistical significance was set at a *p* value of 0.05 for all the tests. The statistical analysis was performed using Graphpad Prism 9.3.1 (Dotmatics, San Diego).

2.5. Viable Cell Assay

S. aureus cultures were grown overnight at 37°C in a shaking incubator. The cultures were shifted to static growth conditions as described previously for the development of biofilms. These biofilm cultures were transferred to a sterile coverslip and treated with p62 for one hour. The biofilms were then stained with propidium iodide (PI) and SYTO[®] 9 from the LIVE/DEAD Biofilm Viability Kit

for screening of viable cells under the confocal microscope. The non-treated and treated cells were stained with PI (10.02 mM/ml) and SYTO[®] 9 (60 mM/ml) for 30 minutes and then washed with sterile Milli-Q water. The samples were observed under a confocal microscope (FV3000, Olympus). The excitation for green channel was kept at 488nm and for the PI fluorescence at 561nm. The images obtained were analysed using the ImageJ software suite (Olympus).

2.6. Visualization in SEM

For visualization of the effect on the microbial biofilm, these were fixed on coverslips by treating with glutaraldehyde for suitable time, before further processing and preparation. Fixed biofilms on the coverslips were washed multiple times with PBS and further treated with 1% osmium tetroxide, to improve the contrast of the images. This was followed by gradual dehydration in graded acetone series to a final concentration of 100% at room temperature. The dehydrated microbial biofilm-containing coverslips were subjected to complete drying by liquid carbon dioxide in a Critical Point Dryer, CPD (EMITECH, K850). All microbial biofilm-containing coverslips after drying, were mounted on stubs or SEM chucks and subjected to sputter coating with gold-palladium in vacuum [35, 36].

Microbial biofilms were imaged using Field Emission Scanning Electron Microscope (FE-SEM QUANTA 200 FEG, Netherland). All treated biofilm samples were observed by the secondary electron scanning mode at high vacuum conditions with 5, 10 and 15 kV of accelerating voltage and images were captured at a magnification range of 5000X, 10000X and 25000X.

3. Results:

The *M. oleifera* leaves, on transfer to an aqueous medium showed the presence of proteinaceous content to the tune of 0.74 mg/ml as determined by the Bradford method. On being subjected to ammonium sulphate fractionation, this yielded a pellet which was rich in protein and a supernatant with very little protein [29]. The ammonium sulphate pellet (fraction P) was resuspended in adequate concentration before being applied to a Superdex-200 column. Further purification in the ion-exchange column showed an elution profile which matched with the single band as visible in the SDS-PAGE (Figure 1).

For the determination of the MIC of the p62 protein, the OD₆₀₀ of *S. aureus* culture was measured at intervals of 6, 12 and 24 hours post treatment with purified p62 protein at different concentrations. At p62 concentrations lower than 100µg, the OD₆₀₀ values were not significantly lesser than that of the control (non-treated) cells (0.5), while for 150µg and 100µg, the values were significantly lower at 0.36 and 0.37, respectively. The positive control (lysostaphin treated cells) showed the lowest OD

of 0.195 while the cells treated with proteinase-K inhibited p62 showed an OD comparable to the non-treated cells. Across the 6, 12 and 24 hour setups, 100µg of p62 showed fair inhibition of growth. Hence, the minimum inhibition concentration for *S. aureus* with p62 appeared to be 100 µg/ml.

The protein p62, which had a determined isoelectric point of 4.7, turned out to be in monomeric form in solution as understood from the oligomeric status determined with gel filtration chromatography (Figure S1). FTIR analysis of the protein fractions showed an Amide I peak at 1650 nm and Amide II peak at 1450 nm (Figure 2).

The purified p62 was extracted from the gel by in-gel tryptic digestion and the subsequent peak mapping using the Spectrum Mill software and the peptide mass fingerprinting yielded the following incomplete sequence having
MTIALGKFTKDENDLFDIMDDWLR.....CGLSKSMDSLGPIENTSISED PVINDTHKNI
HGWGESSSYYSNVDHLVGAK..... The sequence appeared novel with some resemblance to significant identities to the *M. oleifera* chloroplast proteins photosystem II protein D2 (accession id. gi|2050188615|gb|QWL14850.1) (Supplementary Table 1). The false discovery rate (FDR) analysis yielded zero residues.

Thermal stability of the protein, estimated using intrinsic tryptophan fluorescence, showed no discernible shift in the absorption maxima up to a temperature of 50°C. There was an observed reduction of the intensity of the peak from 25°C though as the temperature increased (Figure 3). The p62 thus appeared to be stable till a temperature of 50°C and can be thus sufficiently thermostable at physiological temperatures. The same was observed when the protein was subjected to temperature changes and observed in the CD spectrophotometer. Additionally, CD spectroscopic assignment of the secondary structural data for the protein showed an equivalent prevalence of α helices (36.3%) and β sheets (37.2%) at room temperature.

S. aureus RN322 cells, which were grown in liquid media and then transferred to static culture for biofilm formation, formed a dense layer of biofilm at the surface of the culture tube, which was estimated by staining with crystal violet. Growth was observable in 3 days (0.64), but was significant after 5 days (0.87), as quantified by estimation in a UV-Vis spectrophotometer at 570 nm using the classical estimation method.

Visual comparison of the cultures revealed similar pellicle thicknesses for the untreated biofilm (a), biofilm treated with buffer blank (b) and biofilm treated with p62+proteinase K (c), while the biofilm sample treated with the purified p62 protein (d) had significantly reduced pellicle thickness,

comparable to the biofilm treated with the positive control lysostaphin (e) (Figure 4). The crystal violet binds to the bacterial cell wall and the presence of more cells on the glass tube walls will result in the absorption of more crystal violet by the biofilm. Therefore, it can be safely assumed that the intensity of the crystal violet solution, formed after dissolution in alcohol would be directly proportional to the amount of biofilm sticking to the walls of the tubes (Figure 4a). Quantitatively, the fractions b and c showed equivalent amount of biofilm growth as the control fraction a. In the case of the fraction d, which was treated with 100 micrograms of the purified protein, the reduction in the biofilm was drastic as is evident from the intensities of the bound crystal violet as well as the pellicle pattern on the tubes (Figure 4b). The positive control lysostaphin is a known inhibitor of growth of *S. aureus* and has a MIC of around 2.5 µg, but has been used at a higher concentration to keep an uniformity with the sample p62.

The *S.aureus* cells stained with LIVE/DEAD[®] Biofilm Viability kit, when visualized under the confocal microscope further validated the activity of the p62 protein on biofilms. While SYTO[®] 9 can stain both damaged and healthy cells because of improved membrane permeability, PI can stain only the damaged cells whose membranes have been disrupted [37]. When untreated biofilms were visualized with the PI and SYTO[®] 9 (as described in the manufacturer's protocol) stains under the confocal microscope, mostly green fluorescence was observed, understandably so, as the cocci were healthy and viable. On the other hand, cells in the biofilms which were treated with 100µg of p62 (the MIC) were mostly stained red with propidium iodide. This is a notable indicator of the disruption of the healthy cocci in the biofilm consequent to the treatment with p62 (Figure S2).

For further visualization and validation, the biofilm was transferred to a coverslip after 7 days from initial inoculation in all experiments for the SEM assay. After processing and observation on SEM stubs, a dense biofilm was visualized, with thick bunches of cocci on the coverslip at low magnification (5000X). These were imaged at higher magnification (at 10000X), which revealed the presence of typical cocci of *S. aureus* with the appearance of an exopolysaccharide matrix of biofilm, formed after 7 days of growth (Figure 5a). Growth conditions were maintained similarly to achieve consistent biofilm layers. The transferred biofilm was treated both with the crude extract and the purified p62 and processed for fixing.

The biofilms so formed were initially observed for the activity of the crude extract on them. On imaging under FE-SEM, there was an associated reduction in the distribution and density of the cocci on the coverslips after treatment with the crude *M. oleifera* extract. The plates also showed scattered remnants of coccal bunches, having ragged fragments of exopolysaccharides on them (Figure 5b).

The samples which were treated with 100 µg of the purified protein showed significant detachment of biofilms from the cocci and a pronounced dispersal of the biofilm. The cocci were observed as isolated and scarcely populated bunches (6-7 together) on the plates, with discernible distance from other similar bunches, and devoid of the biofilm attachment. In fact, most stretches of the plate were free of biofilm formation and deformed aggregated remnants of the biofilms could be seen scattered around the plate at 25000X magnification. Additionally, some of the cocci in these treated plates showed considerable deformation and loss of size (Figure 5c).

4. Discussion and Conclusion:

The Gram-positive human commensal, *S. aureus*, has been known to cause chronic infections, when present as biofilm [38-41]. Biofilm formation by *S. aureus* has been often seen as a strategy for survival and propagation of infection by the bacteria [42]. The persistence of the biofilm may be on the tissues of the human host, or on medical implants like prosthetic devices, catheters, etc [43, 44].

In this report, the process of extraction from the *M. oleifera* leaves was concentrated on using the aqueous fraction. The crude extract when applied to *S. aureus* biofilms showed ample signs of disruption of the biofilm, with separation of individual bunches of cocci from the exopolysaccharide matrix. On application of the purified p62 fraction, the biofilm disruption was amplified. The disruption of the biofilm was effective at 100µg of p62, and in some cases, some distortion of coccal morphology was also observed indicative of the effect on the cells. However, the coccal disruption needs to be studied in detail, and this manuscript does not claim to that effect. The study of the cocci treated with the purified extract, under the scanning electron microscope now showed a general lack of the biofilm exopolysaccharide remnants too and the remaining cocci had a rarefied distribution, with 7 or less *S. aureus* cells in a bunch. Generally, the plates which had been treated with the purified fraction showed a relatively clear surface, devoid of much biofilm, but with some sparse traces of cocci and clumps of exopolysaccharide left behind. This was also reinforced by the presence of non-viable cells that were observed in the biofilm treated with p62 and visualized under the confocal microscope.

S. aureus biofilms are a persistent burden on prosthetics and implantation technologies. Bacteria within biofilms are difficult to target with antibiotics or other agents, principally due to the inherent resistance of biofilms to such agents. The leaf extracts of *M. oleifera* being rich in proteinaceous content showed potent activity against *S. aureus* biofilms. The application of the purified 62 kDa protein, with a MIC of 100 µg, displayed a remarkable disruption of the biofilm in general. The bacteria within the biofilm were also shown to be under stress upon application of the protein. While

the protein p62 appears thus to be a potent source of anti-biofilm activity against staphylococcal biofilms, more work needs to be undertaken to devise effective delivery mechanisms of the protein into biofilms formed on surfaces. The incorporation of the p62 onto nano-delivery vehicles might add on to the efficacy of the anti-biofilm activity and can go a long way into the formulation of a possible coating material for prosthetics and implant devices.

Ethics Approval and Consent to Participate

Not Applicable

Human and Animal Rights

Not Applicable

Consent for Publication

All authors have read the manuscript and consented to the publication

Availability of Data and Materials

The material availability has been notified in the manuscript. The material data supporting the findings of the article is available in the Calcutta University Herbarium with reference number CUH/20088.

Funding (Mention grant no.)

The funding for this work is from a grant from ICMR, India numbered OMI/4/2019-ECD-I

Conflict of Interest

The authors declare that all authors have gone through the manuscript and there is no conflict of interest whatsoever.

Acknowledgements

The work undertaken in this publication has been facilitated by a grant from ICMR numbered OMI/4/2019-ECD-I. LM has been supported by a scholarship from the same source.

REFERENCES

- [1] A. Algburi, N. Comito, D. Kashtanov, L.M.T. Dicks, M.L. Chikindas, Control of biofilm formation: Antibiotics and beyond, *Appl. Environ. Microbiol.* 83 (2017) 1–16. <https://doi.org/10.1128/AEM.02508-16>.

- [2] S. Dolatabadi, H.N. Moghadam, M. Mahdavi-Ourtakand, Evaluating the anti-biofilm and antibacterial effects of *Juglans regia* L. extracts against clinical isolates of *Pseudomonas aeruginosa*, *Microb. Pathog.* 118 (2018) 285–289. <https://doi.org/10.1016/j.micpath.2018.03.055>.
- [3] D. Lahiri, S. Dash, R. Dutta, M. Nag, Elucidating the effect of anti-biofilm activity of bioactive compounds extracted from plants, *J. Biosci.* 44 (2019). <https://doi.org/10.1007/s12038-019-9868-4>.
- [4] M. Otto, Staphylococcal Biofilms, *Microbiology Spectrum* 6 (2018) 1–17. <https://doi.org/10.1128/microbiolspec.GPP3-0023-2018>.
- [5] Z. Khatoon, C.D. McTiernan, E.J. Suuronen, T.F. Mah, E.I. Alarcon, Bacterial biofilm formation on implantable devices and approaches to its treatment and prevention, *Heliyon.* 4 (2018) e01067. <https://doi.org/10.1016/j.heliyon.2018.e01067>.
- [6] P.D. Deivamarudachalam Teepica, P. Srinivasan, G. Guna, K. Manimekalai, D. Jaganathan, *in Vitro* Anti Biofilm Activity of *Piper longum* and *Piper nigrum* Against Clinical Isolates of *Streptococcus pyogenes* Isolated From Pharyngitis Patients, *Int. Res. J. Pharm.* 6 (2015) 122–132. <https://doi.org/10.7897/2230-8407.06229>.
- [7] C.R. Arciola, D. Campoccia, P. Speziale, L. Montanaro, J.W. Costerton, Biofilm formation in Staphylococcus implant infections. A review of molecular mechanisms and implications for biofilm-resistant materials, *Biomaterials.* 33 (2012) 5967–5982. <https://doi.org/10.1016/j.biomaterials.2012.05.031>.
- [8] A. Connaughton, A. Childs, S. Dylewski, V.J. Sabesan, Biofilm disrupting technology for orthopedic implants: What's on the horizon?, *Front. Med.* 1 (2014) 1–4. <https://doi.org/10.3389/fmed.2014.00022>.
- [9] S. Kumar, J. Kamboj, Suman, S. Sharma, Overview for Various Aspects of the Health Benefits of *Piper longum* Linn. Fruit, *JAMS J. Acupunct. Meridian Stud.* 4 (2011) 134–140. [https://doi.org/10.1016/S2005-2901\(11\)60020-4](https://doi.org/10.1016/S2005-2901(11)60020-4).
- [10] J.C. Taganna, J.P. Quanico, R.M.G. Perono, E.C. Amor, W.L. Rivera, Tannin-rich fraction from *Terminalia catappa* inhibits quorum sensing (QS) in *Chromobacterium violaceum* and the QS-controlled biofilm maturation and LasA staphylolytic activity in *Pseudomonas aeruginosa*, *J. Ethnopharmacol.* 134 (2011) 865–871. <https://doi.org/10.1016/j.jep.2011.01.028>.
- [11] P. Sankar Ganesh, R. Rai Vittal, In vitro antibiofilm activity of *Murraya koenigii* essential oil extracted using supercritical fluid CO₂ method against *Pseudomonas aeruginosa* PAO1, *Nat. Prod. Res.* 29 (2015) 2295–2298. <https://doi.org/10.1080/14786419.2015.1004673>.
- [12] S. Perumal, R. Mahmud, Chemical analysis, inhibition of biofilm formation and biofilm eradication potential of *Euphorbia hirta* L. against clinical isolates and standard strains, *BMC Complement. Altern. Med.* 13 (2013) 1–8. <https://doi.org/10.1186/1472-6882-13-346>.

- [13] H.A. Farrag, A.E.D.M.S. Hosny, A.M. Hawas, S.A.A. Hagra, O.M. Helmy, Potential efficacy of garlic lock therapy in combating biofilm and catheter-associated infections; experimental studies on an animal model with focus on toxicological aspects, *Saudi Pharm. J.* 27 (2019) 830–840. <https://doi.org/10.1016/j.jsps.2019.05.004>.
- [14] M. Vergara-Jimenez, M.M. Almatrafi, M.L. Fernandez, Bioactive components in *Moringa oleifera* leaves protect against chronic disease, *Antioxidants.* 6 (2017) 1–13. <https://doi.org/10.3390/antiox6040091>.
- [15] E.M.B. Teixeira, M.R.B. Carvalho, V.A. Neves, M.A. Silva, L. Arantes-Pereira, Chemical characteristics and fractionation of proteins from *Moringa oleifera* Lam. leaves, *Food Chem.* 147 (2014) 51–54. <https://doi.org/10.1016/j.foodchem.2013.09.135>.
- [16] J.K. Dzatam, F.K. Touani, V. Kuete, Antibacterial and antibiotic-modifying activities of three food plants (*Xanthosoma mafaffa* Lam., *Moringa oleifera* (L.) Schott and *Passiflora edulis* Sims) against multidrug-resistant (MDR) Gram-negative bacteria, *BMC Complement. Altern. Med.* 16 (2016) 1–8. <https://doi.org/10.1186/s12906-016-0990-7>.
- [17] A.M. de Oliveira, B.A. de Abreu Filho, F. de Jesus Bassetti, R. Bergamasco, R.G. Gomes, Natural Extract of *Moringa oleifera* Leaves Promoting Control of *Staphylococcus aureus* strains biofilm on PVC surface, *Food Bioprocess Technol.* 13 (2020) 1817–1832. <https://doi.org/10.1007/s11947-020-02521-x>.
- [18] A.R. Abdulkadir, M.M. Hasan, M.S. Jahan, Antimalarial, antioxidant, antimicrobial properties of *Moringa Oleifera* Lam: A review, *Aust. J. Crop Sci.* 12 (2018) 905–908. <https://doi.org/10.21475/ajcs.18.12.06.PNE920>.
- [19] L. Gopalakrishnan, K. Doriya, D.S. Kumar, *Moringa oleifera*: A review on nutritive importance and its medicinal application, *Food Sci. Hum. Wellness.* 5 (2016) 49–56. <https://doi.org/10.1016/j.fshw.2016.04.001>.
- [20] S. Saucedo-Pompa, J.A. Torres-Castillo, C. Castro-López, R. Rojas, E.J. Sánchez-Alejo, M. Ngangyo-Heya, G.C.G. Martínez-Ávila, *Moringa* plants: Bioactive compounds and promising applications in food products., *Food Res. Int.* 111 (2018) 438–450. <https://doi.org/10.1016/j.foodres.2018.05.062>.
- [21] E. Husni, E. Badriyya, L. Putri, Y. Aldi, The effect of ethanol extract of moringa leaf (*Moringa oleifera* lam) against the activity and capacity of phagocytosis of macrofag cells and the percentage of leukosit cells of white mice, *Pharmacogn. J.* 13 (2021) 706–712. <https://doi.org/10.5530/pj.2021.13.90>.
- [22] N.F.S. Mohamad Shariff, T. Singgampalam, C.H. Ng, C.S. Kue, Antioxidant activity and zebrafish teratogenicity of hydroalcoholic *Moringa oleifera* L. leaf extracts, *Br. Food J.* 122 (2020) 3129–3137. <https://doi.org/10.1108/BFJ-02-2020-0113>.
- [23] L.A. Al_husnan, M.D.F. Alkahtani, Impact of *Moringa* aqueous extract on pathogenic bacteria and fungi in vitro, *Ann. Agric. Sci.* 61 (2016) 247–250. <https://doi.org/10.1016/j.aoad.2016.06.003>.

- [24] J.R.O. Peixoto, G.C. Silva, R.A. Costa, J. res L. de Sousa Fontenelle, G.H.F. Vieira, A.A.F. Filho, R.H.S. dos F. Vieira, In vitro antibacterial effect of aqueous and ethanolic *Moringa* leaf extracts, *Asian Pac. J. Trop. Med.* 4 (2011) 201–204. [https://doi.org/10.1016/S1995-7645\(11\)60069-2](https://doi.org/10.1016/S1995-7645(11)60069-2).
- [25] A. Connaughton, A. Childs, S. Dylewski, V.J. Sabesan, Biofilm disrupting technology for orthopedic implants: What's on the horizon?, *Front. Med.* 1 (2014) 1–4. <https://doi.org/10.3389/fmed.2014.00022>.
- [26] A.M. De Oliveira, M. Da Silva Férnandes, B.A. De Abreu Filho, R.G. Gomes, R. Bergamasco, Inhibition and removal of staphylococcal biofilms using *Moringa oleifera* Lam. aqueous and saline extracts, *J. Environ. Chem. Eng.* 6 (2018) 2011–2016. <https://doi.org/10.1016/j.jece.2018.02.043>.
- [27] K.T. Mahmood, T. Mugal, I.U. Haq, *Moringa oleifera*: A natural gift-a review, *J. Pharm. Sci. Res.* 2 (2010) 775–781.
- [28] J.G. Onsare, D.S. Arora, Antibiofilm potential of flavonoids extracted from *Moringa oleifera* seed coat against *Staphylococcus aureus*, *Pseudomonas aeruginosa* and *Candida albicans*, *J. Appl. Microbiol.* 118 (2015) 313–325. <https://doi.org/10.1111/jam.12701>.
- [29] B. Moyo, P.J. Masika, A. Hugo, V. Muchenje, Nutritional characterization of *Moringa (Moringa oleifera* Lam.) leaves, *African J. Biotechnol.* 10 (2011) 12925–12933. <https://doi.org/10.5897/ajb10.1599>.
- [30] S. Sahoo, K.M. Raghavendra, S. Biswas, Identification of a proteinaceous component in the leaf of *Moringa oleifera* Lam. with effects on high serum creatinine, *Indian J. Pharm. Sci.* 76 (2014) 78–81.
- [30] M. Liu, X. Wu, J. Li, L. Liu, R. Zhang, D. Shao, X. Du, The specific anti-biofilm effect of gallic acid on *Staphylococcus aureus* by regulating the expression of the *ica* operon, *Food Control.* 73 (2017) 613–618. <https://doi.org/10.1016/j.foodcont.2016.09.015>.
- [31] L. Sjahfirdi, M. Nasikin, Mayangsari, Protein identification using Fourier transform infrared, *Int. J. Res. Rev. Appl. Sci.* 10 (2012) 418–421. http://www.arpapress.com/Volumes/Vol10Issue3/IJRRAS_10_3_06.pdf.
- [32] A. Shevchenko, H. Tomas, J. Havliš, J. V. Olsen, M. Mann, In-gel digestion for mass spectrometric characterization of proteins and proteomes, *Nat. Protoc.* 1 (2007) 2856–2860. <https://doi.org/10.1038/nprot.2006.468>.
- [33] A. Boyd, A. M. Chakrabarty. *Pseudomonas aeruginosa* biofilms: Role of the alginate exopolysaccharide. *J. Ind. Microbiol.*, **1995**, 15, 162–168.
- [34] D. Bandekar, O.P. Chouhan, S. Mohapatra, M. Hazra, S. Hazra, S. Biswas. Putative protein VC0395_0300 from *Vibrio cholerae* is a diguanylate cyclase with a role in biofilm formation, *Microbiol. Res.* 202 (2017) 61–70.

- [35] P. Allan-Wojtas, L. Truelstrup Hansen, A.T. Paulson, Microstructural studies of probiotic bacteria-loaded alginate microcapsules using standard electron microscopy techniques and anhydrous fixation, *LWT - Food Sci. Technol.* 41 (2008) 101–108. <https://doi.org/10.1016/j.lwt.2007.02.003>.
- [36] R. Lamed, J. Naimark, E. Morgenstern, E.A. Bayer, Scanning electron microscopic delineation of bacterial surface topology using cationized ferritin, *J. Microbiol. Methods.* 7 (1987) 233–240. [https://doi.org/10.1016/0167-7012\(87\)90045-5](https://doi.org/10.1016/0167-7012(87)90045-5).
- [37] Rio L, Kusiak-Nejman E, Kiwi J, et al (2012) Comparison of methods for evaluation of the bactericidal activity of copper-sputtered surfaces against methicillin-resistant *Staphylococcus aureus*. *Appl Environ Microbiol* 78:8176–8182. <https://doi.org/10.1128/AEM.02266-12P>.
- [38] Maiti, S. Chatterjee, R. Dey, A. Kundu, R. Dey, Biofilms on indwelling urologic devices: Microbes and antimicrobial management prospect, *Ann. Med. Health Sci. Res.* 4 (2014) 100. <https://doi.org/10.4103/2141-9248.126612>.
- [39] J.P. O’Gara. *ica* and beyond: Biofilm mechanisms and regulation in *Staphylococcus epidermidis* and *Staphylococcus aureus*. *FEMS Microbiol. Lett.* 270 (2007) 179–188. <https://doi.org/10.1111/j.1574-6968.2007.00688.x>
- [40] C. Kranjec, D. Morales Angeles, M. Torrissen Mårli, L. Fernández, P. García, M.Kjos, D.B. Diep. Staphylococcal Biofilms: Challenges and Novel Therapeutic Perspectives. *Antibiotics* 10 (2021) 131. <https://doi.org/10.3390/antibiotics1002013>.
- [41] J.L. Brooks, K.K.Jefferson . Phase Variation of Poly-N-Acetylglucosamine Expression in *Staphylococcus aureus*. *PLoS Pathog.* 10. (2014) <https://doi.org/10.1371/journal.ppat.1004292>
- [42] K. Schilcher, A.R. Horswill. Staphylococcal Biofilm Development: Structure, Regulation, and Treatment Strategies. *Microbial Mol Biol Rev* 84 (2020) e00026-19
- [43] L. Barrett, B. Atkins. The clinical presentation of prosthetic joint infection, *J. Antimicrob. Chemother.* 69 (2014) 25–28. <https://doi.org/10.1093/jac/dku250>
- [44] R.M. Corrigan, D. Rigby, P. Handley, T.J. Foster. The role of *Staphylococcus aureus* surface protein SasG in adherence and biofilm formation. *Microbiology* 153 (2007) 2435–2446. <https://doi.org/10.1099/mic.0.2007/006676-0>

Figure Legends:

Fig. 1 Purification profile of *M. oleifera* leaf aqueous fraction in 10% SDS-PAGE. Lane1: Marker (figures showing molecular weight in kDa), Lane 2: Fraction after partial purification in Superdex, Lane 3: Purified protein fraction after Q HP (ion exchange). Inset: Elution profile after Q HP purification.

Figure 2. Spectral scan of p62 purified protein with IR. The significant amide bands for characteristic understanding of secondary structure of protein through FTIR was obtained at 1650 nm for AmideI and at 1450 nm for AmideII peak.

Fig. 3. Left: Spectral scans of p62 protein at an excitation of 295 nm and emission range of 300 to 450nm. The absorbance intensity dramatically reduces above 25°C and stays consistent at temperature points from 30-60°C. A significant blue shift in the wavelength is observed at temperature beyond 50°C. **Right:** CD spectral analysis of the protein with respect to change of temperature revealed a similar pattern with no perceptible change of spectral pattern till a temperature of 50°C.

Fig. 4 (a) Biofilm formation in 7 day old cultures of *Staphylococcus aureus* after staining with crystal violet. a: control with biofilm growth, b: treatment with p62 digested by proteinase K, c: biofilm with buffer blank, d: biofilm treated with 100 µg of purified protein, e: biofilm treated with 100 µg lysostaphin. (b) The crystal violet bound biofilm was dissolved in 75% ethanol and estimated spectrophotometrically at 570 nm

Figure 5. (a) Biofilm formation of the *Staphylococcus aureus* (magnification 10000X), (b) Coccal density in biofilm (magnification 25000X), (c) Coccal dispersal and biofilm after treatment with crude extract (magnification 25000X), (d) Scarce remnants of biofilm with cocci which have undergone drastic reduction in number as well as change in morphology after treatment with 100 µg purified p62.

Figures:

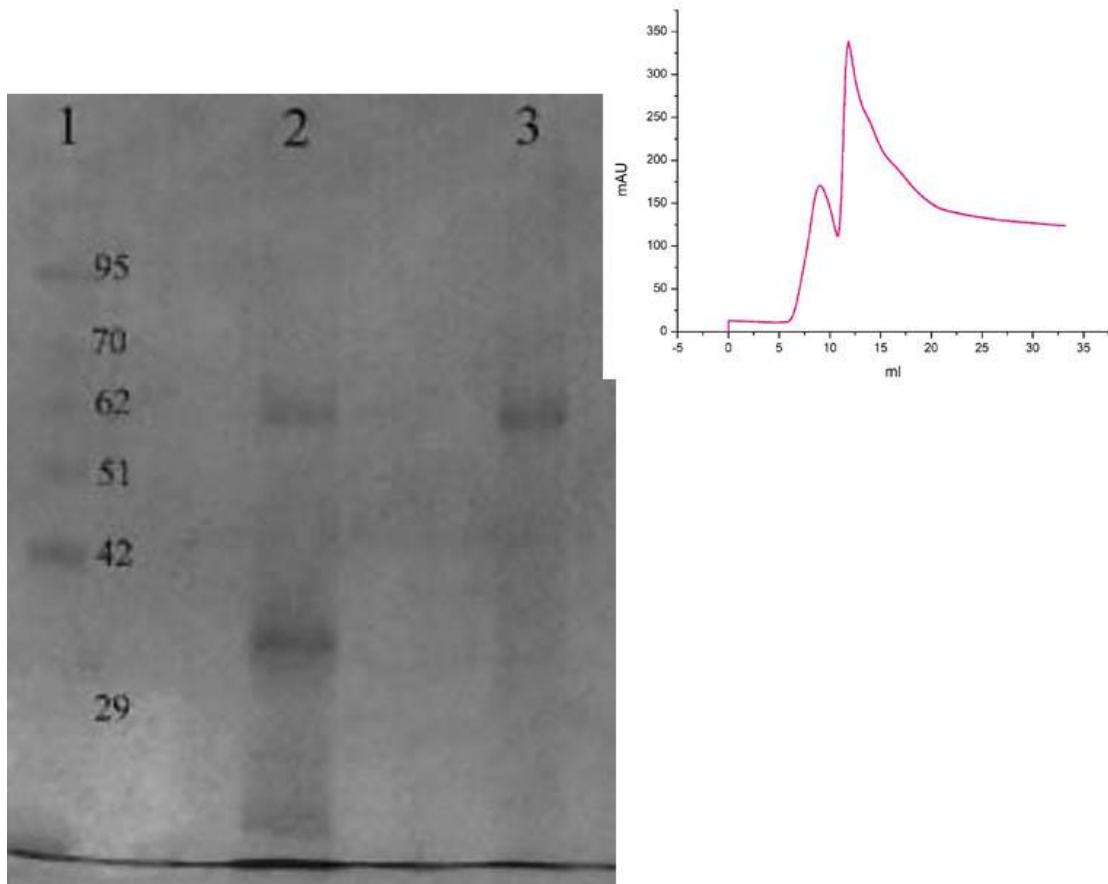


Fig. 1 Purification profile of *M. oleifera* leaf aqueous fraction in 10% SDS-PAGE. Lane1: Marker (figures showing molecular weight in kDa), Lane 2: Fraction after partial purification in Superdex, Lane 3: Purified protein fraction after Q HP (ion exchange). Inset: Elution profile after Q HP purification.

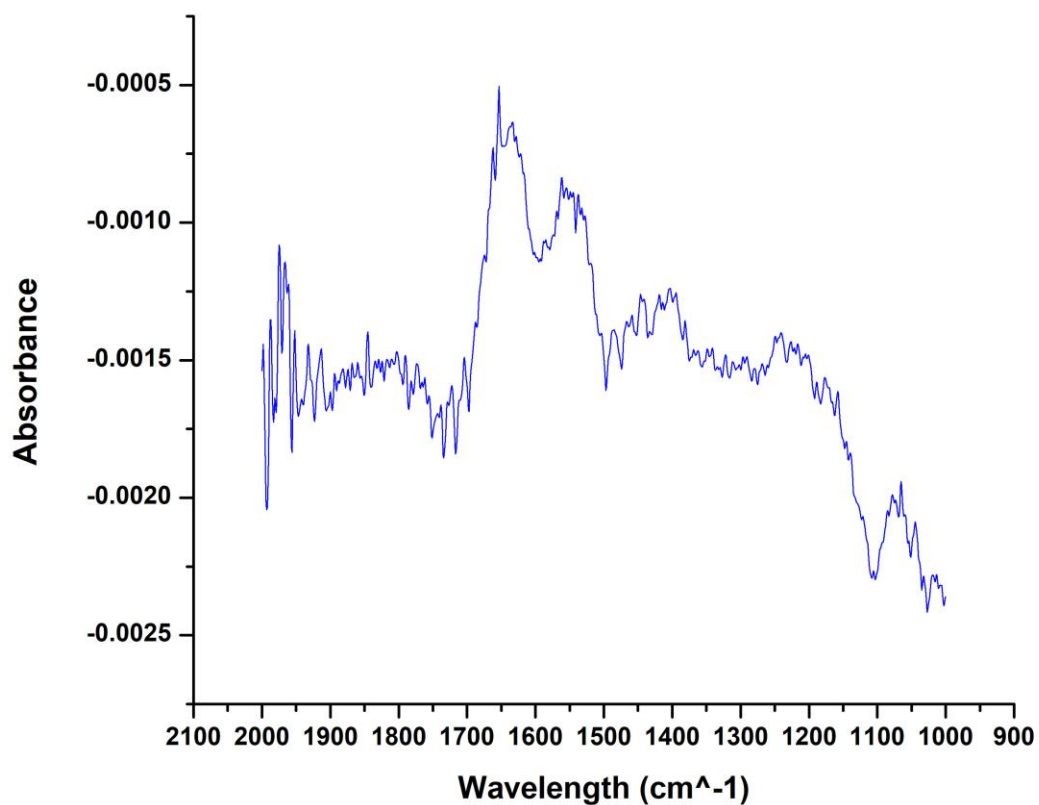


Fig. 2 Spectral scan of p62 purified protein with IR. The significant amide bands for characteristic understanding of secondary structure of protein through FTIR was obtained at 1650 nm for AmideI and at 1450 nm for AmideII peak

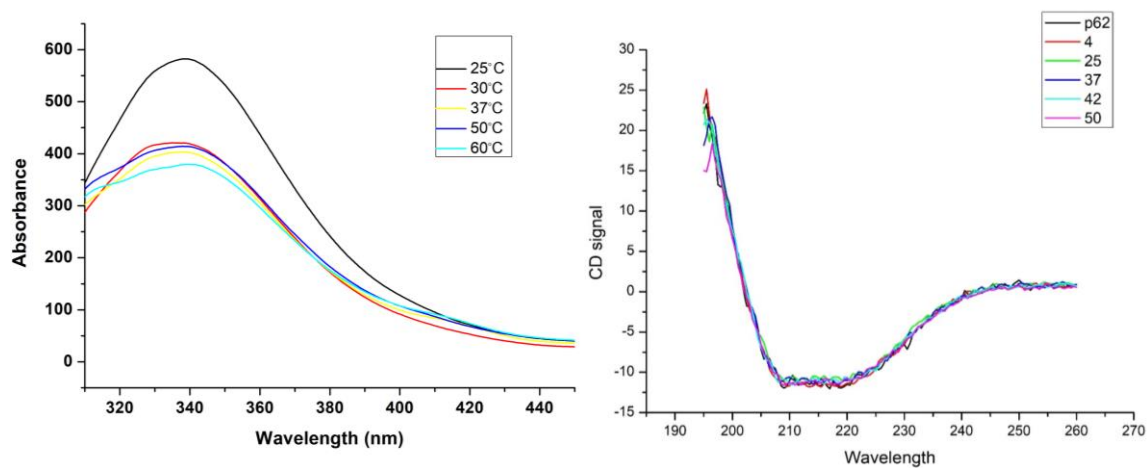


Fig. 3. Left: Spectral scans of p62 protein at an excitation of 295 nm and emission range of 300 to 450nm. The absorbance intensity dramatically reduces above 25°C and stays consistent at temperature points from 30-60°C. A significant blue shift in the wavelength is observed at temperature beyond 50°C. **Right:** CD spectral analysis of the protein with respect to change of temperature revealed a similar pattern with no perceptible change of spectral pattern till a temperature of 50°C.

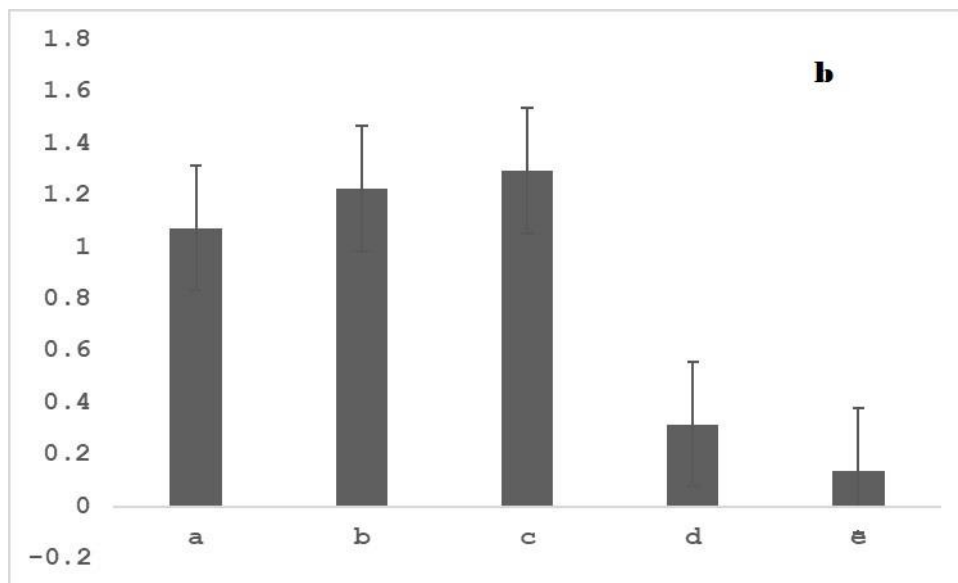
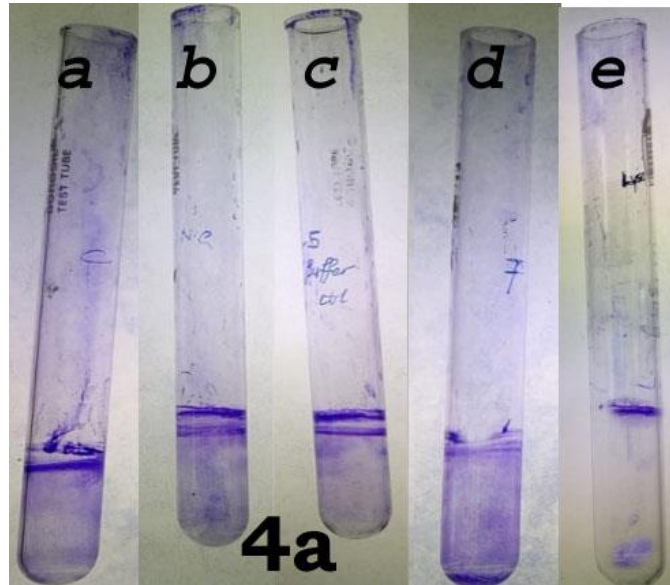


Fig. 4 (a) Biofilm formation in 7 day old cultures of *Staphylococcus aureus* after staining with crystal violet. a: control with biofilm growth, b: treatment with p62 digested by proteinase K, c: biofilm with buffer blank, d: biofilm treated with 100 μ g of purified protein, e: biofilm treated with 100 μ g lysostaphin. (b) The crystal violet bound biofilm was dissolved in 75% ethanol and estimated spectrophotometrically at 570 nm

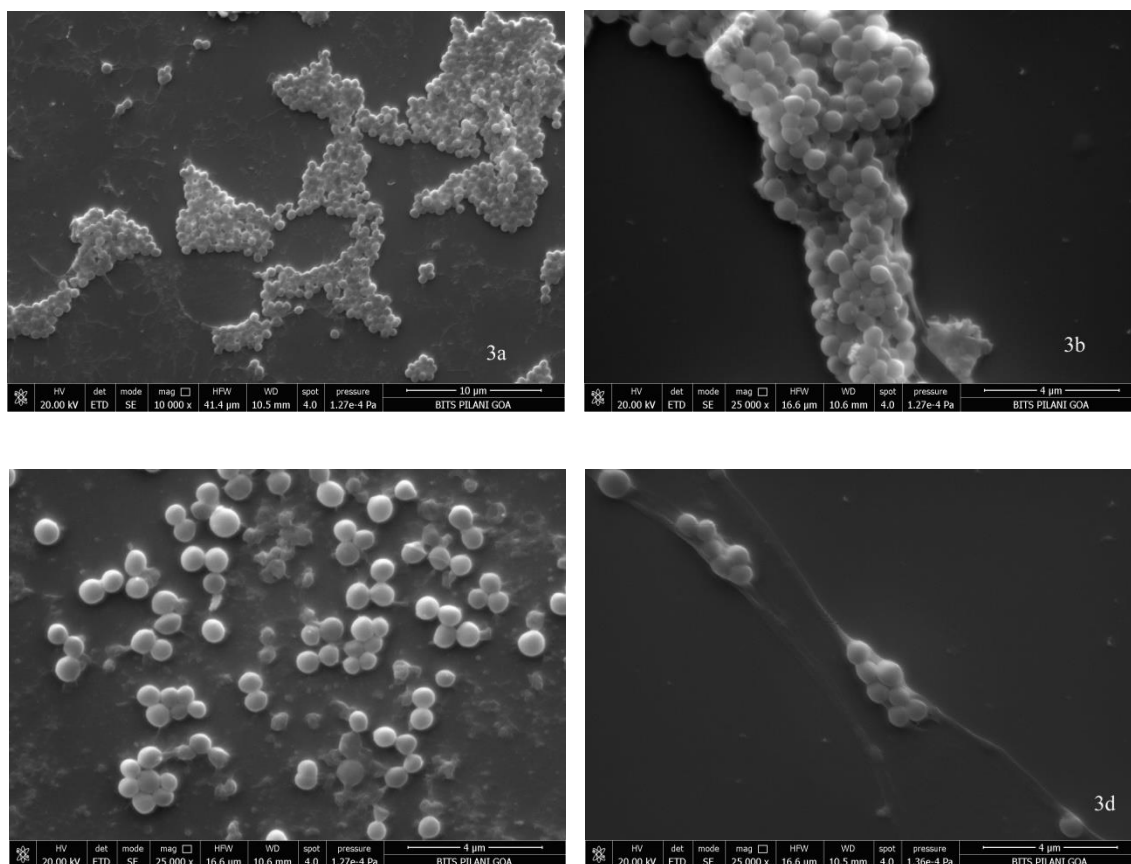


Fig. 5 (a) Biofilm formation of the *Staphylococcus aureus* (magnification 10000X), (b) Coccal density in biofilm (magnification 25000X), (c) Coccal dispersal and biofilm after treatment with crude extract (magnification 25000X), (d) Scarce remnants of biofilm with cocci which have undergone drastic reduction in number as well as change in morphology after treatment with purified p62